Quantum Information Processing (2026) 25:109
https://doi.org/10.1007/s11128-026-05127-y

Graph-encoded strategic interactions in multiplayer quantum games

Michael Tsakiroglou[1] · Ioannis Liliopoulos[1] · Georgios D. Varsamis[1] · Kristin Milchanowski[2,3] · Ioannis G. Karafyllidis[1]

Received: 26 November 2025 / Accepted: 25 February 2026

Abstract

Multiplayer quantum games have received growing attention due to the ability of quantum computational models to access enlarged strategic spaces, thereby enabling the emergence of nonclassical Nash equilibria and Pareto-efficient solutions. Concurrently, graph-theoretic representations have become a standard tool for encoding relational dependencies among interacting players. This work establishes a unified formalism that embeds arbitrary graph topologies into parametrized quantum-game circuits, providing a direct mapping between network structure and the strategic interaction space of quantum players. Within this framework, we analytically and computationally evaluate how graph-induced interpersonal couplings modulate payoff distributions over repeated quantum-game iterations. In addition, we integrate a reward-driven adaptation algorithm that allows players to optimize their local strategy parameters dynamically with respect to accumulated payoffs. Experimental results demonstrate that the equilibrium reward landscape is highly sensitive to the players' graph-theoretic centrality and the weighted structure of their adversarial and cooperative relationships.

✉ Ioannis G. Karafyllidis
ykar@ee.duth.gr

Michael Tsakiroglou
tskmichalis@gmail.com

Ioannis Liliopoulos
ililiopo@ee.duth.gr

Georgios D. Varsamis
gevarsam@ee.duth.gr

Kristin Milchanowski
kristin.milchanowski@bmo.com

1 Department of Electrical and Computer Engineering, Democritus University of Thrace, Kimmeria, Xanthi 67100, Greece

2 Bank of Montreal (BMO), Montreal, QC, Canada

3 Said Business School, University of Oxford, Oxford, UK

Published online: 23 March 2026

Keywords Quantum computing · Quantum games · Quantum algorithms · Graph encoding

1 Introduction

Quantum information science has undergone rapid development over the past decade, propelled by advances in coherent control, circuit-based architectures, and hybrid quantum–classical computational models. Quantum algorithms such as those of Deutsch [1], Grover [2], and Shor [3] have established that quantum processors can exploit superposition, interference, and entanglement to access computational regimes that are inaccessible to classical computers, whether operated as standalone quantum platforms [4–6] or integrated into variational hybrid workflows [7–9]. As noise levels decrease and system sizes scale upward, understanding how quantum resources modify established models of information processing, including strategic and decision-theoretic formalisms, has become an increasingly significant direction within the quantum information community [10, 11].

Game theory offers a formal framework for analyzing strategic interactions among rational players. In its classical formulation, equilibria arise from fixed-point conditions on mixed strategies, and payoff structure is constrained to classical probability distributions [12–15]. When generalized to the quantum domain, however, the strategic landscape acquires fundamentally new features: players act on local subsystems of a composite Hilbert space, strategies may be represented as unitary operations, and correlations between players can be encoded through entangled resource states or entangling gates. These ingredients enable quantum strategies that lack classical counterparts and can induce qualitatively different equilibrium spaces. The seminal demonstrations of quantum advantage in strategic settings—including Meyer's quantum coin-flip protocol [16], the Eisert–Wilkens–Lewenstein (EWL) quantization of the Prisoner's Dilemma [17, 18], and Benjamin Hayden's extension to multipartite scenarios [19]—established the foundations of multiplayer quantum-game theory. Since then, characterizing the operational role of nonclassical correlations, circuit structure, and entanglement depth in strategic dynamics has remained a central research question [20]. Multiplayer quantum games exhibit qualitatively new features that are absent in the two-player setting. Most notably, the entanglement structure becomes substantially richer, enabling genuinely multipartite correlations that cannot be decomposed into pairwise interactions. As a consequence, the strategic landscape is significantly more complex: each player's payoff depends on collective quantum correlations shared among all participants, rather than solely on the actions of individual opponents. [21–24]

Graph-theoretic models are extensively used in contemporary quantum information research. They arise naturally in the study of entanglement structures, multipartite resource states, quantum error-correcting codes, and distributed quantum networks. A graph, consisting of a vertex set and an edge set [25, 26], provides a compact representation of pairwise interaction patterns. From Euler's classical formulation of the Königsberg bridge problem [27] to applications in complex systems [28–30],

graphs have provided a formal language for encoding structural constraints that directly impact computational and operational capabilities.

In this work, we investigate multiplayer quantum games in which the interaction topology among players is explicitly encoded by an underlying graph. We model players as subsystems of a composite Hilbert space and introduce an entangling operator whose structure is determined by an undirected, unweighted graph. This construction embeds the graph's topology directly into the quantum-game circuit, enabling a controlled study of how structural properties, such as local degree, centrality, and global connectivity, shape payoff distributions and strategic equilibria. To capture adaptive behavior across repeated rounds, we incorporate the EXP3 algorithm [31, 32], a canonical method for adversarial multi-armed bandits, to update each player's mixed unitary strategy based on observed payoff statistics. All protocols are implemented using ideal state vector simulations within the Qiskit framework [33], and evaluated on several representative graph families, including Barabási–Albert [34] and Erdős–Rényi [35] networks, which serve as standard models of heterogeneous and stochastic connectivity in both quantum and classical network theory [36].

2 Two-player quantum games

We begin by revisiting the quantum formulation of the classical Prisoner's Dilemma introduced by Eisert et al. [17, 18] and its experimental realization [37]. The corresponding two-player quantum circuit, shown in Fig. 1, consists of two qubits, one for each player, an entangling operator $\hat{E}$, individual strategy operators $\hat{U}_0$ and $\hat{U}_1$, and the adjoint operator $\hat{E}\dagger$. The operators $\hat{U}_0$ and $\hat{U}_1$ encode the strategic choices of the two players. In the quantum setting, any single-qubit unitary is, in principle, a valid strategy.

To ensure that the classical game is embedded as a special case of the quantum game, as required in standard quantization frameworks [38], we map the classical strategies "cooperate" and "defect" to their quantum analogues using the Identity and Pauli-X gates, given in (1) and (2), respectively.

$$I = \begin{bmatrix} 1 & 0 \\ 0 & 1 \end{bmatrix} \tag{1}$$

$$X = \begin{bmatrix} 0 & 1 \\ 1 & 0 \end{bmatrix} \tag{2}$$

Throughout this work, the entangling operator $\hat{E}$ takes the form defined in Eq. (3).

$$\hat{E} = \exp\left(-i\frac{\gamma}{2}X \otimes X\right) = \begin{bmatrix} \cos(\frac{\gamma}{2}) & 0 & 0 & -i\sin(\frac{\gamma}{2}) \\ 0 & \cos(\frac{\gamma}{2}) & -i\sin(\frac{\gamma}{2}) & 0 \\ 0 & -i\sin(\frac{\gamma}{2}) & \cos(\frac{\gamma}{2}) & 0 \\ -i\sin(\frac{\gamma}{2}) & 0 & 0 & \cos(\frac{\gamma}{2}) \end{bmatrix} \tag{3}$$

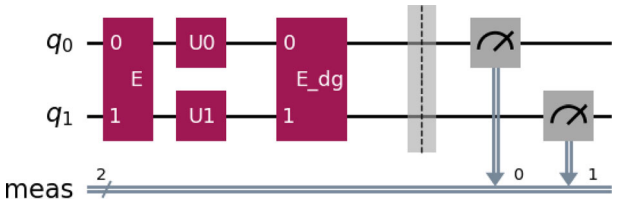

Fig. 1 Setup of a two-player quantum game. The E and $E\dagger$ notations correspond to the entanglement and adjoint entanglement operators and the U_i to the i_{th} player's strategy

Table 1 General payoff matrix for the two-players quantum game

	$\|00\rangle$	$\|01\rangle$	$\|10\rangle$	$\|11\rangle$
Player 0	$p_{0,\|00\rangle}$	$p_{0,\|01\rangle}$	$p_{0,\|10\rangle}$	$p_{0,\|11\rangle}$
Player 1	$p_{1,\|00\rangle}$	$p_{1,\|01\rangle}$	$p_{1,\|10\rangle}$	$p_{1,\|11\rangle}$

Table 2 Payoff matrix used in this work

	$\|00\rangle$	$\|01\rangle$	$\|10\rangle$	$\|11\rangle$
Player 0	3	0	5	1
Player 1	3	5	0	1

with $\gamma \in [0, \frac{\pi}{2}]$. This operator was initially introduced by Eisert [17, 18] and has been further analyzed in [21]. In this work, the parameter γ has been set equal to $\frac{\pi}{2}$. After this, the $\hat{E}$ operator is given by:

$$\hat{E} = \exp\left(-i\frac{\pi}{4}X \otimes X\right) = \begin{bmatrix} \frac{\sqrt{2}}{2} & 0 & 0 & -i\frac{\sqrt{2}}{2} \\ 0 & \frac{\sqrt{2}}{2} & -i\frac{\sqrt{2}}{2} & 0 \\ 0 & -i\frac{\sqrt{2}}{2} & \frac{\sqrt{2}}{2} & 0 \\ -i\frac{\sqrt{2}}{2} & 0 & 0 & \frac{\sqrt{2}}{2} \end{bmatrix} \tag{4}$$

Since our study focuses on repeated pairwise interactions among many players, each two-player interaction is modeled as an independent quantum game. Payoffs for these pairwise games are computed using the general two-player quantum payoff matrix proposed in [21] and presented in Table 1. We adopt the classical Prisoner's Dilemma parameters for the underlying payoff values, resulting in the matrix shown in Table 2. The expected payoff for each player in a single round is computed according to Eq. (5).

$$\begin{aligned} P_i = {} & p_{i,|00\rangle}|\langle 00||\psi_m\rangle|^2 + p_{i,|01\rangle}|\langle 01||\psi_m\rangle|^2 + p_{i,|10\rangle}|\langle 10||\psi_m\rangle|^2 \\ & + p_{i,|11\rangle}|\langle 11||\psi_m\rangle|^2 \end{aligned} \tag{5}$$

where $i \in [0, 1]$ for the two-player game and $|\psi_m\rangle$ is the measured state at the end of each game.

3 Quantum games in networks

3.1 Model formulation

Let $G = (V, E)$ be an undirected graph with $|V| = n$ nodes, representing the set of players in a multiplayer quantum game. As discussed in the Introduction, the graph encodes the interaction structure among agents: in a star graph, the central node interacts with all peripheral nodes, in a ring, each node interacts with its two neighbors, and in Barabási–Albert or Erdős–Rényi networks, high-degree nodes engage with many other nodes simultaneously.

In many graphs, a node participates in multiple edges. To model these relationships explicitly, we associate two qubits with each edge $\{u, v\} \in E$, treating every edge as a distinct two-player quantum game. Thus, a graph with $|E|$ edges corresponds to a quantum circuit with $2|E|$ qubits. This formulation allows each player to select different local strategies for different neighbors, thereby capturing heterogeneous or edge-specific behaviors across the network. For each player u, we denote by Q_u the set of qubits assigned to that player within the full circuit. To determine this set, we initially sort all edges $\{u, v\} \in E$ of the graph, in ascending order, according to the beginning node u. Then, for each edge $\{u, v\} \in E_{\text{sorted}}$, we distribute the available qubits to each player alternatively, in ascending order, with respect the player's id. For example, in the ring graph, demonstrated in Fig. 2a, E_{sorted} is $\{\{0, 1\}, \{0, 3\}, \{1, 2\}, \{2, 3\}\}$. For the edge $\{0, 1\}$, we assign qubit q_0 to player 0 and q_1 to player 1. Similarly, for the edge $\{0, 3\}$, we assign qubit q_2 to player 0 and q_3 to player 3. This process is performed until all the qubits of the quantum circuit are distributed to the competing players.

To investigate how a player's choice toward one opponent influences their behavior toward others, we introduce a graph entanglement operator, $\hat{E}_{\text{Graph}}$, which encodes all pairwise relationships in the network. Construction of this operator proceeds by iterating through all edges of the graph. For each edge $\{u, v\}$, we entangle the qubit of player u associated with that edge with all qubits assigned to player v that correspond to other edges, and vice versa. In this manner, $\hat{E}_{\text{Graph}}$ couples the strategic subsystems of each pair of connected players, while simultaneously propagating correlations across the broader network. The operator is formally defined in Eq. (6).

$$\hat{E}_{Graph} = \exp\left(-i\frac{\pi}{4} \sum_{<u,v>\in E} \sum_{\substack{q_j \in Q_{u\to v} \\ q_k \in Q_{nc}}} X_{q_j} \otimes X_{q_k}\right), \\ \{q_j, q_k | (q_j \notin Q_u \wedge q_k \notin Q_u) \vee (q_j \notin Q_v \wedge q_k \notin Q_v)\} \tag{6}$$

where $Q_{u\to v}$ contains the pair of qubits that are assigned to the edge $(u \to v)$ and $Q_{nc} = (Q_u - Q_{u\to v}) \cup (Q_v - Q_{u\to v})$ contains the qubits of both players that are not assigned to the edge $(u \to v)$. Additionally, in Eq. (6), terms X_{q_j} and X_{q_k} are associated with the application of the Pauli X operator to all qubits q_j and q_k that fall within groups $Q_{u\to v}$ and Q_{nc}, respectively.

To clarify, let us consider the ring graph as depicted in Fig. 2a, as a test case. For this example, we focus on nodes 0 and 1, which are connected to each other through

the edge $(0 \rightarrow 1)$. Nodes 0 and 1 will be players 0 and 1 in the quantum game. Also, we assume that Player 0 is assigned with the qubit set $Q_0 = \{q_0, q_2\}$ and Player 1 with the $Q_1 = \{q_1, q_4\}$, in the quantum circuit, since both nodes are linked to two other nodes in the graph. The qubits that correspond to this edge are q_0 and q_1 and so $Q_{0\rightarrow 1} = \{q_0, q_1\}$. Similarly, $Q_{nc} = (Q_0 - Q_{0\rightarrow 1}) \cup (Q_1 - Q_{0\rightarrow 1}) = \{q_2, q_4\}$. According to Eq. (6), considering only the $(0 \rightarrow 1)$ edge, the graph entanglement operator will be:

$$\hat{E}_{G_{0\rightarrow 1}} = \exp\left(-i\frac{\pi}{4}\sum_{\substack{q_j \in Q_{0\rightarrow 1} \\ q_k \in Q_{nc}}} X_{q_j} \otimes X_{q_k}\right) = \exp\left(-i\frac{\pi}{4}(X_{q_0} \otimes X_{q_4} + X_{q_1} \otimes X_{q_2})\right) \quad (7)$$

We repeat this process for all edges $(u \rightarrow v) \in E$ to obtain the $\hat{E}_{\text{Graph}}$ for the entire graph.

Regarding the quantum game, each player may exploit one of the following single-qubit operators as his strategy:

$$U = \{I, H, X, Y, Z\}.$$

whereas I and H correspond to the Identity and Hadamard gates and X, Y, and Z to the three Pauli gates. In round t, each player i applies the $U_i^{(t)} \in U$ strategy to q_i. The steps to construct the corresponding quantum circuit are described in Algorithm 1:

Algorithm 1 Quantum games circuit construction

Obtain and sort, in ascending order, all the undirected edges $\{u, v\}$ of the graph.
Create a quantum circuit comprising $2|E|$ qubits.
Assign to each player its corresponding set of qubits of the quantum circuit.
Create the graph entanglement operator $\hat{E}_{Graph}$, relying on Eq. (6), and apply it to all qubits.
for each i-th edge $\{u, v\} \in E$: **do**
  Apply the entanglement operator $\hat{E}$, as described in Eq. (4), to both (q_{2i}, q_{2i+1}) qubits.
  Apply each player's strategy U to his corresponding qubit.
  Apply the disentanglement operator $\hat{E}^{\dagger}$ to both qubits.
end for
Apply the graph disentanglement operator $\hat{E}^{\dagger}_{Graph}$ to all qubits.
Measure all qubits on the Z computational basis and compute each player's payoffs.

This process should be repeated for each round of the quantum game.

Let us consider again the four-node ring graph, as an example of how a graph may be transformed into a quantum-game circuit, using the aforementioned algorithm. The ring graph illustrated in Fig. 2a contains four undirected edges, sorted as $\{(0, 1), (0, 3), (1, 2), (2, 3)\}$. According to (1) each jth edge is assigned a qubit pair (q_{2j}, q_{2j+1}). The qubits assigned to each player are as follows:

$$Player_0 : \{q_0, q_2\}, \quad Player_1 : \{q_1, q_4\}, \quad Player_2 : \{q_5, q_6\}, \quad Player_3 : \{q_3, q_7\}.$$

Additionally, the graph entanglement $\hat{E}_{\text{Graph}}$ operator for this example is presented in Fig. 3, both in its' block form (Fig. 3a) and in its' decomposed structure (Fig. 3b).

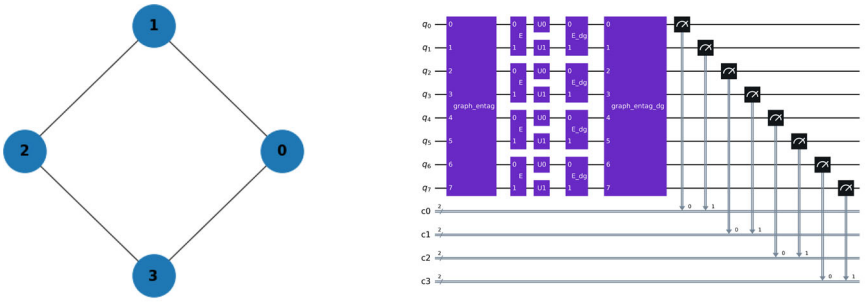

(a) 4-node ring graph. (b) Quantum circuit produced by our algorithm.

Fig. 2 A four-player graph mapped to a quantum circuit. In this case, a ring graph, depicted in Fig. 2a, with players $p_0, ..., p_3$ is mapped to the quantum circuit in Fig. 2bcomprising qubits $q_0, ..., q_7$. This circuit consists of the graph entanglement $\hat{E}_{\text{Graph}}$ and disentanglement $\hat{E}^{\dagger}$ operators together with four intermediate two-qubit sub-circuits related to the graph's edges. Each of these sub-circuits comprises an entanglement operator $\hat{E}$, the players' strategies U and a disentanglement $E^{\dagger}$ operator

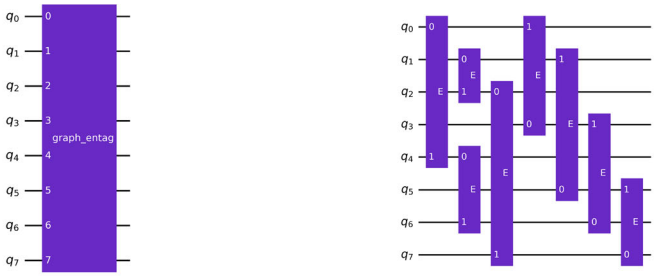

(a) Four node ring graph entanglement operator. (b) Decomposition of the graph entanglement operator.

Fig. 3 Graph entanglement operator for the four-node ring example

3.2 Experimental framework

To complement the structural analysis of the circuit, we integrate an adaptive strategy-selection mechanism, enabling players to update their strategies based on observed payoffs throughout the experiment. Inspired by the adversarial multi-armed bandit setting, each player is treated as an autonomous player whose goal is to maximize cumulative reward over repeated game rounds.

Each player u is assigned a weight vector

$$W = \{W_{u \to v} \in \mathbb{R}^{K}_{>0} \mid (u \to v) \in \mathcal{A}\}$$

where K is the number of available quantum strategies and $\mathcal{A} = \{(u \to v), (v \to u) \mid \{u, v\} \in E\}$ is the set of directed edges. Although the underlying graph is undirected, directed edge labels allow us to maintain separate strategy distributions for each player–neighbor pair. All weights are initialized to 1, corresponding to uniform priors over the strategy set.

Players update their strategy weights via the EXP3 algorithm, which adjusts the probability distribution over strategies based on each player's payoff differences during game rounds. For every experiment, we perform 10 independent repetitions of each quantum game, each consisting of 7000 rounds. The complete experimental procedure is summarized in Algorithm 2.

Algorithm 2 Experimental procedure algorithm

Input: Graph $G = (V, E)$ with $|V| = n$; rounds T; experiments M;
strategy set $U = \{I, X, Y, H, Z\}$; Quantum circuit qc
Output: Weight history HistW; Final weights FinalW;
Payoff history HistP

Initialize $K \leftarrow |U|$
Set hyperparameters (η, γ) for the EXP3 algorithm
for $m \leftarrow 1$ To M **do** ▷ for each experiment
  $W_{u\to v} = 1$, for each $(u \to v) \in \mathcal{A}$ ▷ Initialize weights
  Initialize output vectors HistW, FinalW, HistP
  Initialize P and S. ▷ Payoffs and Strategies vectors
  for $t \leftarrow 1$ To T **do**
    $W_{norm} \leftarrow \{\frac{W_{u\to v}}{\|W_{u\to v}\|_1} \in \mathbb{R}^K_{>0} \mid (u \to v) \in \mathcal{A}\}$ ▷ Normalize weights
    $p = (1-\gamma)W_{norm} + \frac{\gamma}{K}\mathbf{1}_K$ ▷ Probability to select each strategy
    $S \leftarrow Select\_Optimal\_Strategies(p, U)$
    $P(t) \leftarrow Play\_Quantum\_Game(G, qc, S)$ ▷ Obtain players' payoffs
    $\widehat{r}_i = \frac{P(t)_i}{p[S_i]}, i \in [0, n]$ ▷ Player estimated reward for his set of strategies S
    $W[S_i] \leftarrow W[S_i] \exp\left(\frac{\gamma}{K}\widehat{r}_i\right), i \in [0, n]$ ▷ Update weights
    $HistW[m, t] \leftarrow W_{norm}$
    $HistP[m, t] \leftarrow P(t)$
  end for
  $FinalW[m] \leftarrow \{\frac{W_{u\to v}}{\|W_{u\to v}\|_1} \in \mathbb{R}^K_{>0} \mid (u \to v) \in \mathcal{A}\}$
end for

In each round, every player samples strategies for each edge $(u \to v) \in A$ according to their current probability distribution directly related to their weight values. A quantum circuit is then constructed using these strategies, executed, and the resulting payoffs are recorded. After each round, all players update their weight vectors following the EXP3 update rules. Across all repetitions, we record the temporal evolution of each player's weights and payoffs using the lists $HistW$ and $HistP$, respectively.

4 Research outcomes

We conducted experiments on four representative graph topologies, i.e., star, ring, Barabási–Albert, and Erdős–Rényi—each containing seven nodes, as shown in Fig. 4. For each graph type, we performed experiments both with and without the graph entanglement operator $\hat{E}_{\text{Graph}}$ in order to isolate its influence on strategy evolution and payoff distribution. This comparative analysis reveals how topology-dependent quantum correlations shape the strategic behavior of players and the resulting equilibrium structure.

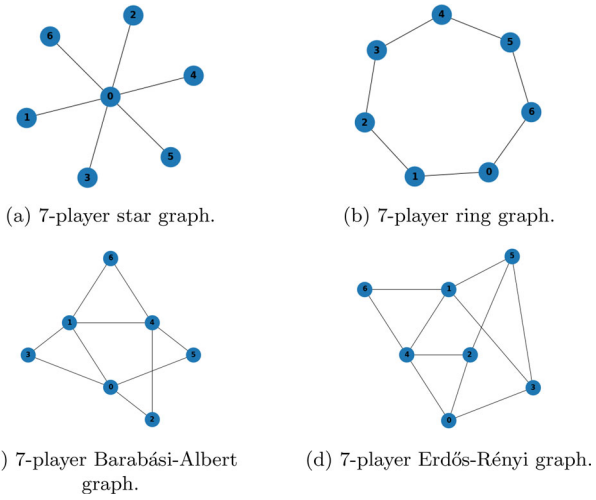

(a) 7-player star graph.

(b) 7-player ring graph.

(c) 7-player Barabási-Albert graph.

(d) 7-player Erdős-Rényi graph.

Fig. 4 Four graphs considered for our experiments

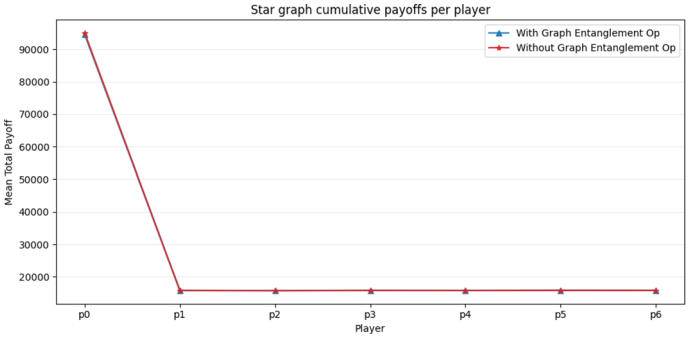

Fig. 5 Cumulative payoff values per player in the star graph

4.1 Star graph

Figure 5 shows the mean cumulative payoffs across ten independent experimental runs. As expected for star topologies, the presence or absence of $\hat{E}_{\text{Graph}}$ has negligible impact on the aggregate outcomes. This is expected since the central node is connected to every other node in the graph and thus it competes in all games that take place on this graph. However, all other players, which participate in a single game, against the central node, will approximately have the same cumulative payoff at the end of the experiments.

Additionally, in Fig. 6 the mean final weights of each player's strategy, against each of his opponents, are presented. We observe that, when $\hat{E}_{\text{Graph}}$ is utilized, all players tend to evenly leverage all possible strategies against their opponents. On the other hand, when $\hat{E}_{\text{Graph}}$ is not used, all players opt for I and Y instead of the X,Z, and H gates as strategies against their opponents. Last but not least, in Fig. 7aand

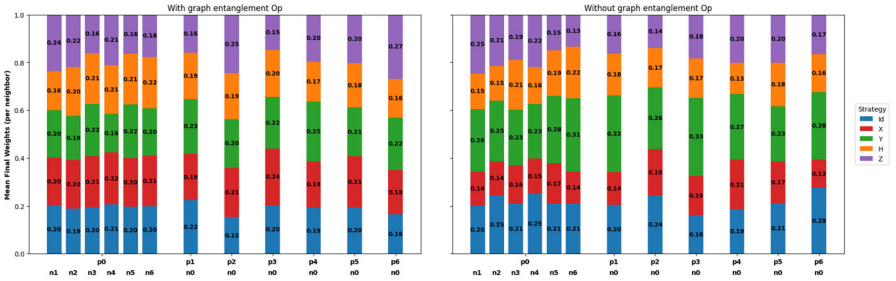

(a) (b)

Fig. 6 Mean final weights of each player's strategy, for each of his n_i opponents, for the star graph. Each bar demonstrates the final weight distribution for the five available strategies player p_i may use against his n_i opponent. **a** With the application of the graph entanglement operator. **b** Without the application of the graph entanglement operator

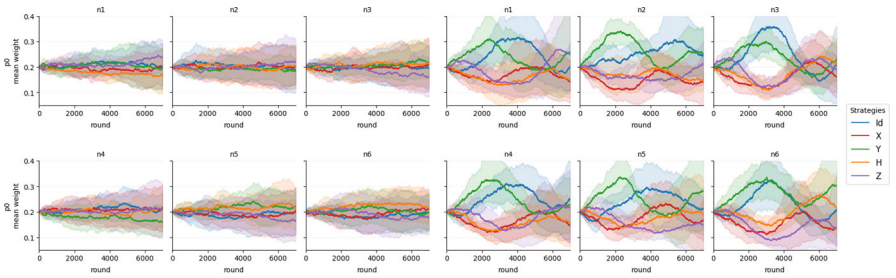

(a) (b)

Fig. 7 Evolution of player 0 strategy weights over successive game rounds, for each of his n_i opponents, **a** with and **b** without the use of the $\hat{E}_{\text{Graph}}$

b , the evolution of the strategies weight values throughout the game's rounds, for player 0, i.e., the central network node, is demonstrated, with and without the $\hat{E}_{\text{Graph}}$ application, respectively. It is evident that the application of $\hat{E}_{\text{Graph}}$ in the quantum circuit yields a more smooth and balanced evolution compared to its absence, which leads to a great variance in all weight values, as the game rounds evolve. Similar behavior is exhibited in the other player's weight evolution diagrams, which may be found in Appendix A.

4.2 Ring graph

For the ring topology, the cumulative payoff distribution (Fig. 8) exhibits a qualitatively different pattern from the star case. When $\hat{E}_{\text{Graph}}$ is included, all players converge toward nearly identical mean cumulative payoffs, consistent with the fact that each node participates in exactly two games. This indicates that the entangling correlations effectively symmetrize the adaptive landscape, enabling all players to approach comparable long-run performance. In contrast, without $\hat{E}_{\text{Graph}}$, pronounced discrepancies arise between players' cumulative payoffs, despite the uniform node degrees. This

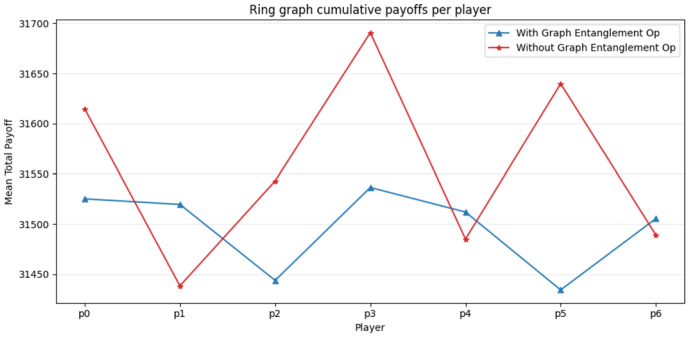

Fig. 8 Cumulative payoff values per player in the ring graph

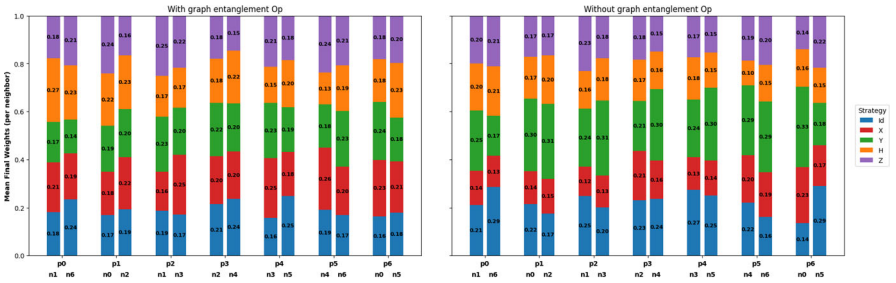

Fig. 9 Mean final weights of each player's strategy, for each of his n_i opponents, for the ring graph. Each bar demonstrates the final weight distribution for the five available strategies player p_i may use against his n_i opponent. **a** With the application of the graph entanglement operator. **b** Without the application of the graph entanglement operator

suggests that, absent the additional inter-edge correlations, the dynamics can amplify local asymmetries in early-round outcomes.

Concerning the ring graph, the cumulative payoff values of the players are demonstrated in Fig. 8. In contrast with the corresponding cumulative values in the star graph, in the ring graph the values obtained differ from each other for different implementations considered. The presence of $\hat{E}_{\text{Graph}}$ in the quantum circuit leads to more reasonable and smaller differences between the mean total payoff of each player. This is something to be expected, since all players compete in exactly two games. So, we await that after a number of rounds, and as players keep adjusting their weights, and therefore their strategies, to achieve better payoffs, all players will converge to approximately the same mean total payoff. However, if $\hat{E}_{\text{Graph}}$ is not used, the differences between the mean total payoffs of all players are considerable.

Figure 9a and b shows that the presence of $\hat{E}_{\text{Graph}}$ again drives the strategy-weight distributions toward near-uniformity, whereas its absence yields the now-familiar bias toward gates I and Y as the players' most common strategy.

As before, the use of $\hat{E}_{\text{Graph}}$ results in a balanced evolution of all players' weights as presented in Fig. 10a. In contrast, when this operator is not used, we notice again many weight value imbalances throughout the experiments, as presented in Fig. 10b.

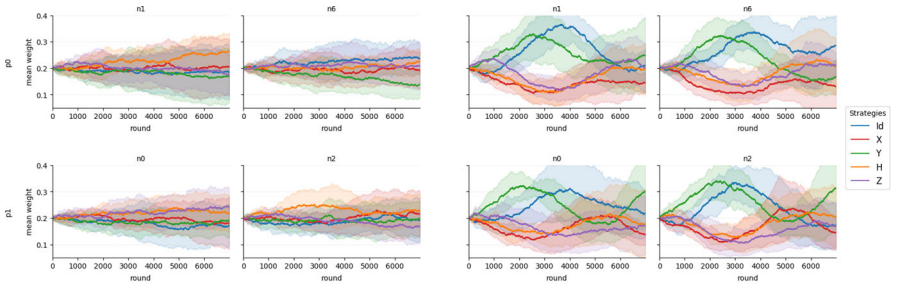

(a) (b)

Fig. 10 Evolution of players 0 and 1 strategy weights over successive game rounds, for each of their n_i opponents, **a** with and **b** without the use of the $\hat{E}_{\text{Graph}}$

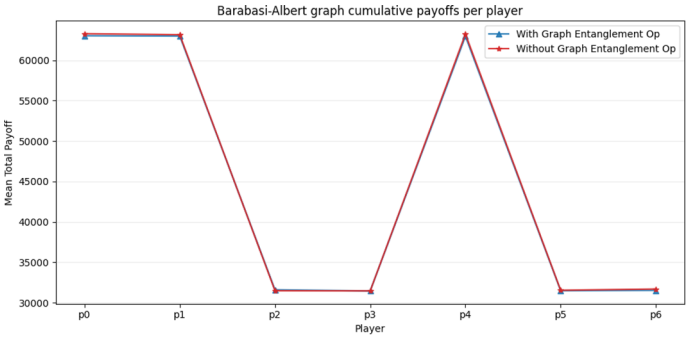

(a)

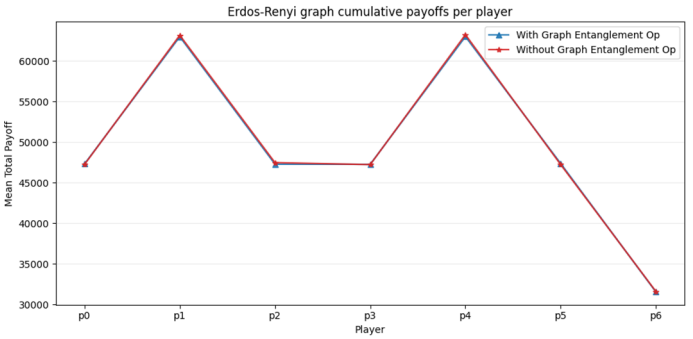

(b)

Fig. 11 Cumulative payoff values per player in **a** Barabási–Albert and **b** Erdős–Rényi graph

In these figures, the evolution of all strategy weights of players 0 and 1 is demonstrated, respectively. The figures presenting the evolution of all strategy weights of the remaining five players may be found in the Appendix.

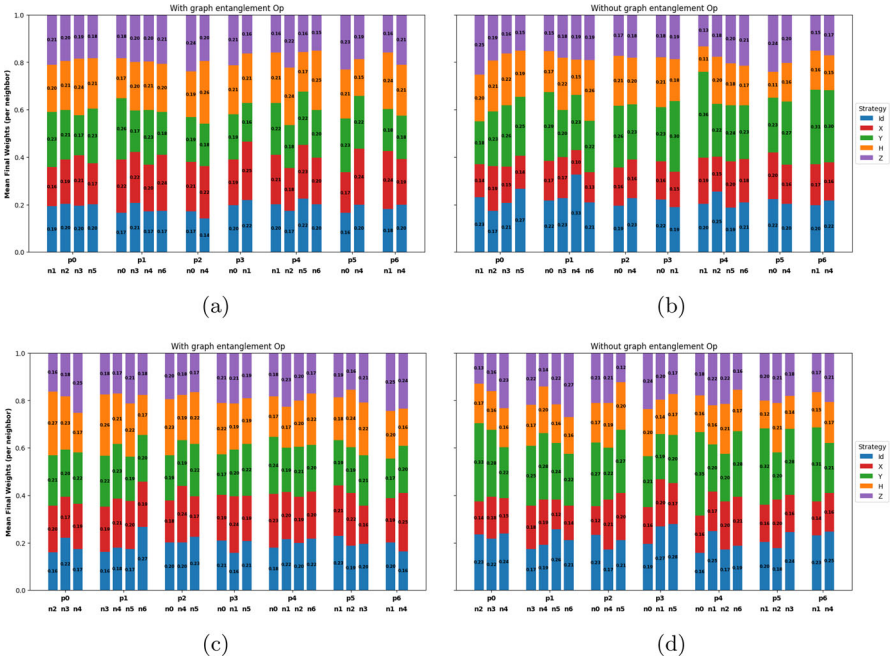

Fig. 12 Mean final weights of each player's strategy, for each of his n_i opponents, for the ring graph. Each bar demonstrates the final weight distribution for the five available strategies player p_i may use against his n_i opponent. **a**, **b** With and without the application of $\hat{E}_{\text{Graph}}$, for the Barabási–Albert graph. **c**, **d** With and without the application of $\hat{E}_{\text{Graph}}$, for the Erdős–Rényi graph

4.3 Barabási–Albert & Erdos–Rényi graphs

The Barabási–Albert and Erdős–Rényi graphs are widely used in graph theory. In this work, they are used to express the relationship between players competing in quantum games. In both these graphs, the players' degrees range from two to four and therefore each player participates in two games minimum. So, we expect that the higher degree nodes, i.e., players that compete in more quantum games, will acquire higher total payoff values compared to lower degree ones. Indeed, this is the case, as presented in Fig. 11.

From the Barabási–Albert-related diagram (11a) we observe that players 0, 1, and 4 have the highest cumulative payoff values. All these nodes have a degree value equal to four, the highest in the graph. Similarly, for the Erdős–Rényi graph (11b) the total payoff of each player is proportional to his degree in the graph; players 1 and 4 obtain the highest payoffs due to participating in more quantum games, whereas all other players reach lower total playoff values at the end of the experiments. Additionally, like in the star graph case, the cumulative payoff values of all players are almost identical, with and without the $\hat{E}_{\text{Graph}}$ application.

Next, in Fig. 12, we display the mean final weights of each player's strategy, against each of his opponents, with and without the use of $\hat{E}_{\text{Graph}}$ for both the Barabási–Albert

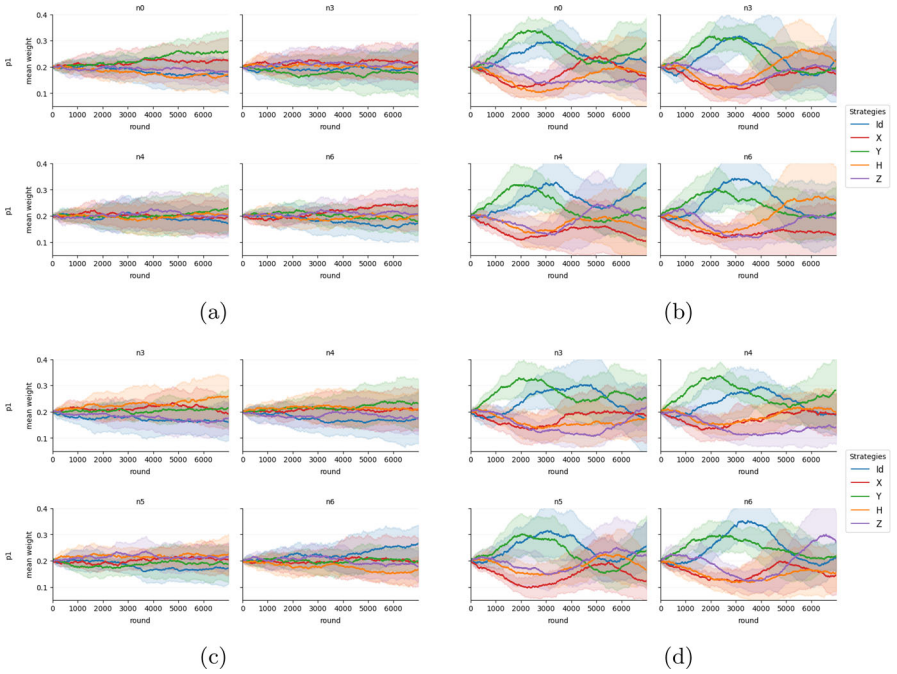

Fig. 13 Evolution of players 0 and 1 strategy weights during successive game rounds, for each of their n_i opponents, **a** with and **b** without the use of the $\hat{E}_{\text{Graph}}$

(Fig. 12a, b) and Erdős-Rényi (Fig. 12c, d) graphs. In both cases, the final weight distribution of each player is similar to the ones presented earlier, for the star and ring graphs. In particular, the presence of the $\hat{E}_{\text{Graph}}$ leads to an equal distribution of strategy choices for each player, whereas its absence causes a shift toward quantum gates Y and I as the dominant strategies of each player against its opponents.

As in all other graph cases considered, the evolution of all strategy weights of each player follow the same pattern. Specifically, when $\hat{E}_{\text{Graph}}$ is used in the quantum-game circuit, the aforementioned weight values exhibit minor fluctuations during the course of the game rounds compared to the case when $\hat{E}_{\text{Graph}}$ is not applied in the quantum circuit. For both these graphs, the evolution of all strategy weights of player 1, i.e., a four-degree node, is demonstrated in Fig. 13. The evolution diagrams of all the other players are presented in the Appendix.

5 Conclusions and future work

In this work, we investigated how graph-encoded interaction topologies influence strategic behavior and payoff distributions in multiplayer quantum games. By introducing the entangling operator $\hat{E}_{\text{Graph}}$, whose structure is directly determined by an underlying undirected and unweighted graph, we provided a systematic method for embedding relational constraints into the quantum-game circuit. We further developed

a quantum algorithm that incorporates this operator into arbitrary multiplayer game instances. To model adaptive strategic behavior across repeated rounds, we integrated the EXP3 adversarial bandit algorithm, enabling each player to update their local unitary strategy in response to observed payoff fluctuations.

Our numerical experiments demonstrate that the presence of $\hat{E}_{\text{Graph}}$ significantly alters the strategic landscape. For graph topologies with uniform degree, the operator induces a more homogeneous evolution of players' strategy weights and yields a more balanced cumulative payoff distribution. Across all investigated graph families, we observe that the payoff obtained by each player is strongly correlated with their graph-theoretic position, nodes with higher degree systematically accumulate greater rewards, highlighting the operational impact of local connectivity in quantum strategic interactions. These results underscore the role of graph topology as a resource that shapes both equilibrium structure and strategic adaptation in quantum games.

A key contribution of this work is the introduction of a general and easily extensible framework that embeds arbitrary relational structures, encoded as graphs, into multiplayer quantum-game circuits. This provides a principled approach for modeling strategic interactions in settings where correlations, influence, or communication constraints are inherent, including domains such as distributed decision-making, multiplayer optimization, and networked social or economic systems

The present study relied on ideal state vector simulations due to the large number of repeated game rounds required for statistical evaluation. A natural direction for future research is to assess the robustness of our framework on real noisy intermediate-scale quantum (NISQ) hardware, as well as on noise-model simulators, to determine how decoherence and gate infidelities affect topology-dependent strategic dynamics. Furthermore, our current analysis is limited to undirected and unweighted graphs. Extending the framework to incorporate weighted and directed edges, thereby encoding asymmetric influence, heterogeneous coupling strengths, or directional information flow, would provide a richer and more expressive entanglement operator $\hat{E}_{\text{Graph}}$. Such generalizations would enable the study of more realistic interaction structures and broaden the applicability of graph-structured quantum games within the quantum information sciences.

Appendix

In this section, we include the additional players' weight evolution figures, for all graphs considered in this work (Figs. 14, 15, 16, 17).

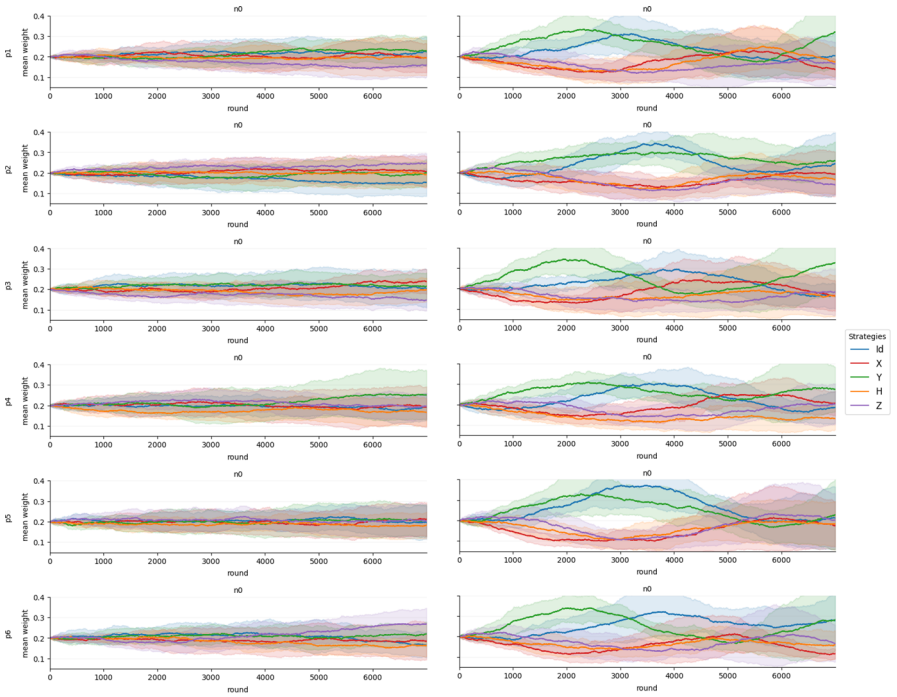

Fig. 14 Evolution of players 1–6 strategy weights over successive game rounds, for each of their n_i opponents, **a** with and **b** without the use of the $\hat{E}_{\text{Graph}}$, for the star graph. Each of these players has a degree value equal to one, meaning that he participates in only one game. Additionally, all players 1–6 play against the same opponent, i.e., player 0

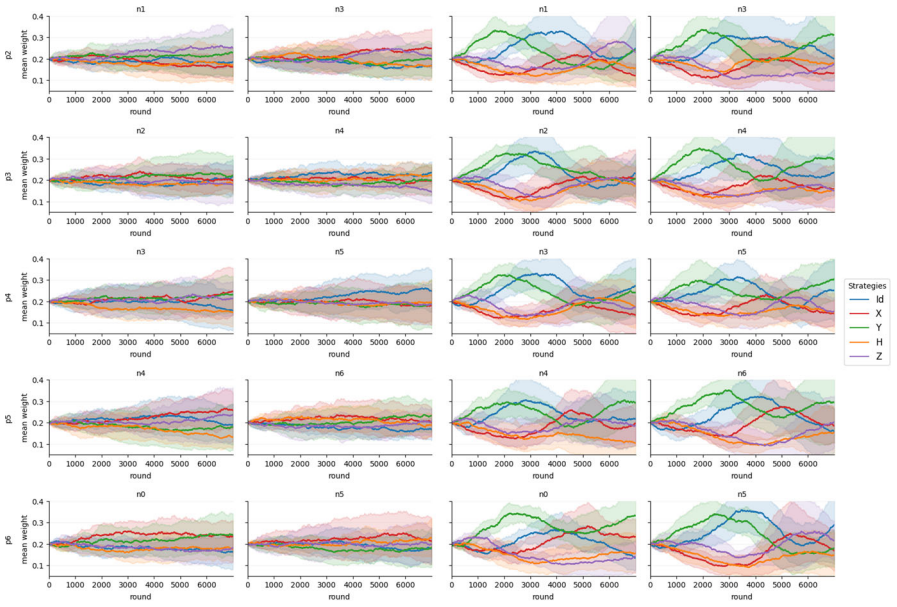

(a) (b)

Fig. 15 Evolution of players 2–6 strategy weights over successive game rounds, for each of their n_i opponents, **a** with and **b** without the use of the $\hat{E}_{\text{Graph}}$, for the ring graph. Each of these players has a degree value equal to two, meaning that he participates in two games

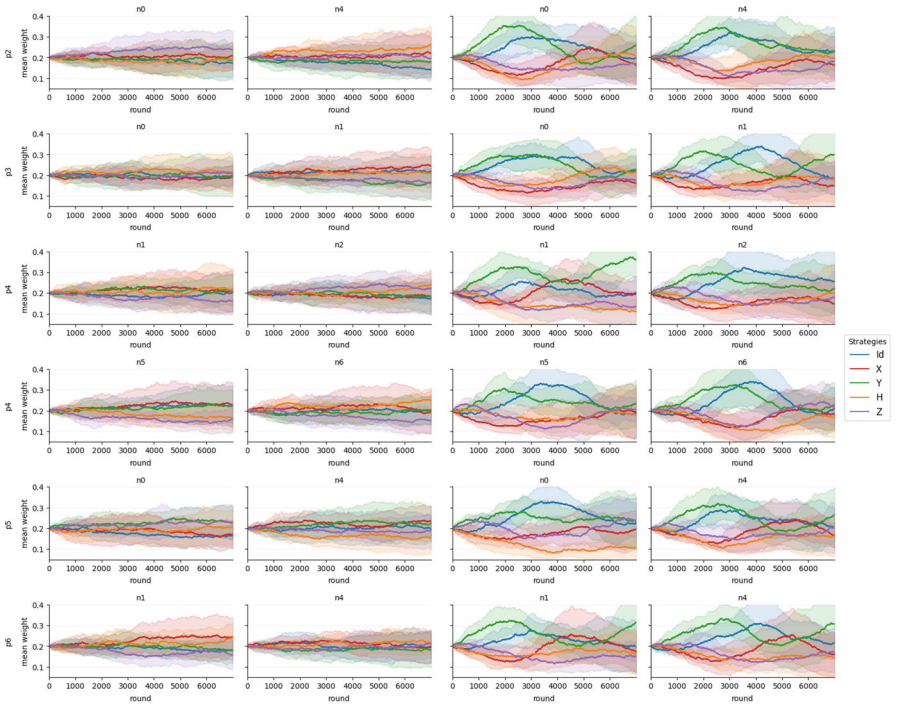

Fig. 16 Evolution of players 2–6 strategy weights over successive game rounds, for each of their n_i opponents, **a** with and **b** without the use of the $\hat{E}_{\text{Graph}}$, for the Barabási–Albert graph. Each of these players has a degree value equal to either two or four, accordingly

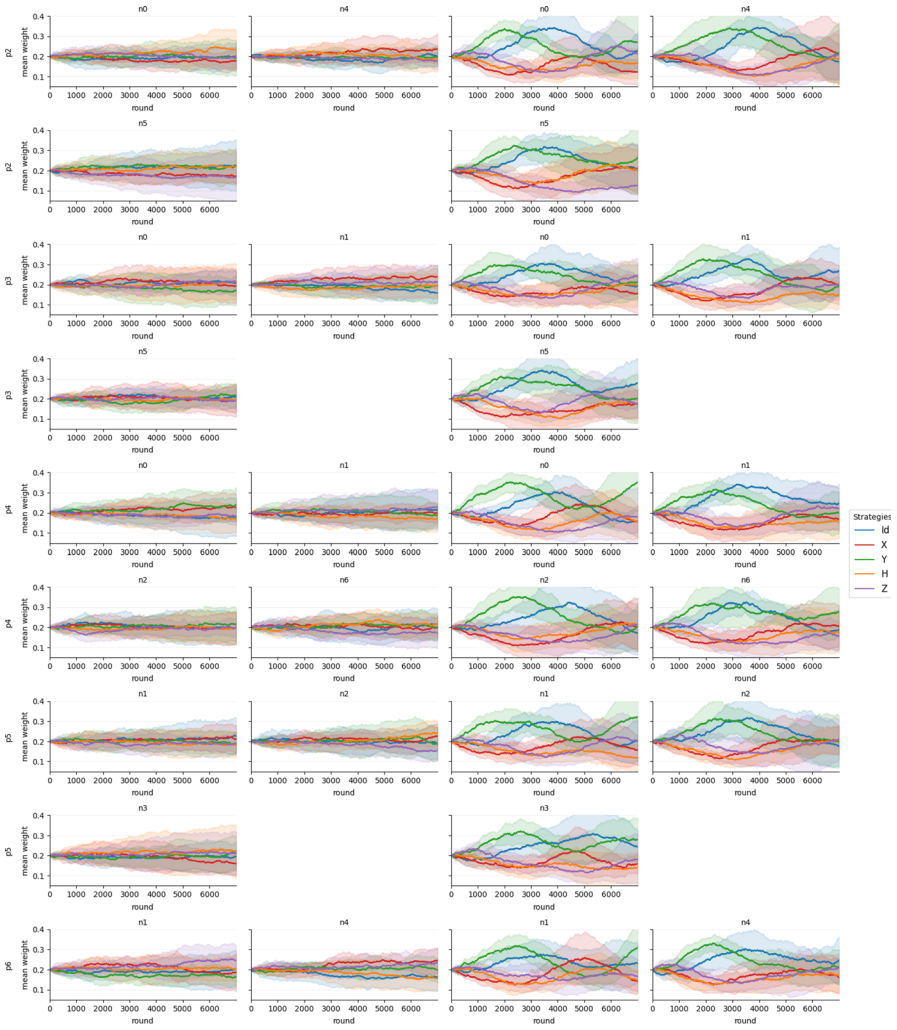

(a) (b)

Fig. 17 Evolution of players 2–6 strategy weights over successive game rounds, for each of their n_i opponents, **a** with and **b** without the use of the $\hat{E}_{\text{Graph}}$, for the Erdős–Rényi graph. Each of these players has a degree value that ranges from two to four, accordingly

Author Contributions All authors contributed equally.

Funding Open access funding provided by HEAL-Link Greece.

Data Availability No datasets were generated or analyzed during the current study.

Declarations

Conflict of interest The authors declare that they have no Conflict of interest.

References

1. Deutsch, D., Jozsa, R.: Rapid solution of problems by quantum computation. Proc. R. Soc. Lond. A **439**, 553–558 (1992)
2. Grover, L.K.: A fast quantum mechanical algorithm for database search. In: Proceedings of the Twenty-eighth Annual ACM Symposium on Theory of Computing, pp. 212–219 (1996)
3. Shor, P.W.: Algorithms for quantum computation: discrete logarithms and factoring. In: Proceedings 35th Annual Symposium on Foundations of Computer Science, pp. 124–134 (1994). IEEE
4. Robert, A., Barkoutsos, P.K., Woerner, S., Tavernelli, I.: Resource-efficient quantum algorithm for protein folding. npj Quantum Inf. **7**(1), 38 (2021)
5. Bauer, B., Bravyi, S., Motta, M., Chan, G.K.L.: Quantum algorithms for quantum chemistry and quantum materials science. Chem. Rev. **120**(22), 12685–12717 (2020)
6. Varsamis, G.D., Karafyllidis, I.G., Gilkes, K.M., Arranz, U., Martin-Cuevas, R., Calleja, G., Wong, J.: Quantum gate algorithm for reference-guided DNA sequence alignment. Comput. Biol. Chem. **107**, 10759 (2023)
7. Bravyi, S., Kliesch, A., Koenig, R., Tang, E.: Hybrid quantum-classical algorithms for approximate graph coloring. Quantum **6**, 678 (2022)
8. Wang, A., Hu, J., Zhang, S., Li, L.: Shallow hybrid quantum-classical convolutional neural network model for image classification. Quantum Inf. Process. **23**, 18145 (2024)
9. Liliopoulos, I., Varsamis, G.D., Milchanowski, K., Martin Cuevas, R., Safouri, K., Dimitrakis, P., Karafyllidis, I.G.: Hybrid classical-quantum multilayer neural networks for monitoring agricultural activities using remote sensing data. Quantum Mach. Intell. **7**(1), 4 (2025)
10. Hallgren, S.: Polynomial-time quantum algorithms for Pell's equation and the principal ideal problem. J ACM (JACM) **54**(1), 1–19 (2007)
11. Arute, F., Arya, K., Babbush, R., Bacon, D., Bardin, J.C., Barends, R., Biswas, R., Boixo, S., Brandao, F.G., Buell, D.A.: Quantum supremacy using a programmable superconducting processor. Nature **574**(7779), 505–510 (2019)
12. Osborne, M.J.: Introduction to Game Theory. Oxford University Press, Oxford, UK (2004)
13. Colman, A.M.: Game Theory and Its Applications: In the Social and Biological Sciences. Psychology Press, Hove, UK (2013)
14. Tadelis, S.: Game Theory: an Introduction. Princeton University Press, Princeton, NJ (2013)
15. Mendelson, E., Zwillinger, D.: Introducing Game Theory and Its Applications. Chapman and Hall/CRC, New York (2024)
16. Meyer, D.A.: Quantum strategies. Phys. Rev. Lett. **82**(5), 1052 (1999)
17. Eisert, J., Wilkens, M., Lewenstein, M.: Quantum games and quantum strategies. Phys. Rev. Lett. **83**(15), 3077 (1999)
18. Eisert, J., Wilkens, M., Lewenstein, M.: Erratum: Quantum games and quantum strategies [phys. rev. lett. 83, 3077 (1999)]. Phys. Rev. Lett. **124**, 139901 (2020).https://doi.org/10.1103/PhysRevLett.124.139901
19. Benjamin, S.C., Hayden, P.M.: Multiplayer quantum games. Phys. Rev. A **64**(3), 030301 (2001)
20. Flitney, A.P., Abbott, D.: Quantum version of the Monty hall problem. Phys. Rev. A **65**(6), 062318 (2002)
21. Varsamis, G.D., Liliopoulos, I., Mohammadbagherpoor, H., Kostopoulos, A.K., Milchanowski, K., Karamatskos, E.T., Dimitrakis, P., Padbury, R.P., Karafyllidis, I.G.: Analysis of the effect of entanglement operators and the scalability of players' payoff computation in n-player quantum games. Adv. Quantum Technol. **8**, e00375 (2025)

22. Zhou, J., Ma, L., Li, Y.: Multiplayer quantum games with continuous-variable strategies. Phys. Lett. A **339**(1), 10–17 (2005)
23. Sousa, P.B.M., Ramos, R.V.: Multiplayer quantum games and its application as access controller in architecture of quantum computers. Quantum Inf. Process. **7**(2), 125–135 (2008)
24. Varsamis, G.D., Liliopoulos, I., Mohammadbagherpoor, H., Kostopoulos, A.K., Milchanowski, K., Karamatskos, E.T., Dimitrakis, P., Padbury, R.P., Karafyllidis, I.G.: Proxy quantum games. Parallel Process. Lett. **35**(03n04), 2550014 (2025)
25. Diestel, R.: Graph Theory, vol. 173. Springer, Berlin (2025)
26. Gross, J.L., Yellen, J., Anderson, M.: Graph Theory and Its Applications. Chapman and Hall/CRC, New York (2018)
27. Euler, L.: Leonhard euler and the königsberg bridges. Sci. Am. **189**(1), 66–72 (1953)
28. Sporns, O.: Graph theory methods: applications in brain networks. Dialogues Clin. Neurosci. **20**(2), 111–121 (2018)
29. Tang, L., Liu, H.: Graph mining applications to social network analysis. In: Managing and Mining Graph Data, pp. 487–513. Springer, Berlin (2010)
30. He, S., Xiong, S., Ou, Y., Zhang, J., Wang, J., Huang, Y., Zhang, Y.: An overview on the application of graph neural networks in wireless networks. IEEE Open J. Commun. Soc. **2**, 2547–2565 (2021)
31. Auer, P., Cesa-Bianchi, N., Fischer, P.: Finite-time analysis of the multiarmed bandit problem. Mach. Learn. **47**(2), 235–256 (2002)
32. Auer, P., Cesa-Bianchi, N., Freund, Y., Schapire, R.E.: The nonstochastic multiarmed bandit problem. SIAM J. Comput. **32**(1), 48–77 (2002)
33. Javadi-Abhari, A., Treinish, M., Krsulich, K., Wood, C.J., Lishman, J., Gacon, J., Martiel, S., Nation, P.D., Bishop, L.S., Cross, A.W., et al.: Quantum computing with qiskit. arXiv preprint arXiv:2405.08810 (2024)
34. Albert, R., Barabási, A.-L.: Statistical mechanics of complex networks. Rev. Mod. Phys. **74**(1), 47 (2002)
35. Erdős, P., Rényi, A.: On random graphs i. Publ. Math. Debrecen **6**(290–297), 18 (1959)
36. Wilson, C., Sala, A., Puttaswamy, K.P., Zhao, B.Y.: Beyond social graphs: user interactions in online social networks and their implications. ACM Transact. Web (TWEB) **6**(4), 1–31 (2012)
37. Altintas, A.A., Ozaydin, F., Bayindir, C., Bayrakci, V.: Prisoners' dilemma in a spatially separated system based on spin–photon interactions. Photonics **9**(9) (2022)
38. Silva, A., Zabaleta, O.G., Arizmendi, C.M.: Maximizing local rewards on multi-agent quantum games through gradient-based learning strategies. Entropy **25**(11), 1484 (2023)